

Comparison of geostatistical approaches to spatially interpolate month-year rainfall for the Hawaiian Islands

Abby G. Frazier,^{a*} Thomas W. Giambelluca,^a Henry F. Diaz^b and Heidi L. Needham^a

^a Department of Geography, University of Hawai'i at Mānoa, Honolulu, HI, USA

^b NOAA/ESRL/CIRES, University of Colorado Boulder, CO, USA

ABSTRACT: The Hawaiian Islands have one of the most spatially diverse rainfall patterns on earth. Knowledge of these patterns is critical for a variety of resource management issues and, until now, only long-term mean monthly and annual rainfall maps have been available for Hawai'i. In this study, month-year rainfall maps from January 1920 to December 2012 were developed for the major Hawaiian Islands. The maps were produced using climatologically aided interpolation (CAI), where the station anomalies were interpolated first, and then combined with the mean maps. A geostatistical method comparison was performed to choose the best interpolation method. The comparison focuses on three kriging algorithms: ordinary kriging (OK), ordinary cokriging (OCK), and kriging with an external drift (KED). Two covariates, elevation and mean rainfall, were tested with OCK and KED. The combinations of methods and covariates were compared using cross-validation statistics, where OK produced the lowest error statistics. Station anomalies for each month were interpolated using OK and combined with the mean monthly maps to produce the final month-year rainfall maps.

KEY WORDS kriging; monthly rainfall; Hawai'i; anomalies; cross-validation

Received 7 January 2015; Revised 30 May 2015; Accepted 8 June 2015

1. Introduction

Precipitation climatologies are very important to research in hydrology, terrestrial ecosystem processes, regional climate, and regional impacts of global change. Understanding rainfall patterns is essential for water resources planning, especially in places where water is scarce and highly dependent on local rainfall. Island communities are particularly sensitive to changes in climate, and accurate data are vital for policy decisions and resource management plans to cope with these effects. In the Hawaiian Islands, a diverse terrain, as well as varied wind patterns and a persistent trade wind inversion (TWD), lead to extremely complex rainfall patterns. Achieving an accurate representation of these patterns is a difficult task, even with a relatively dense network of stations.

The recently completed 'Rainfall Atlas of Hawai'i' (Giambelluca *et al.*, 2013, <http://rainfall.geography.hawaii.edu/>) has produced mean rainfall maps for the seven major islands of Hawai'i. Mean monthly and annual maps depict the average spatial rainfall patterns. The new maps supersede a previous Rainfall Atlas (Giambelluca *et al.*, 1986) in which spatial rainfall patterns were estimated subjectively from point measurements. The most recent project used a Bayesian data fusion method to combine rain gauge data with radar rainfall estimates, mesoscale meteorological model output (MM5), Parameter-elevation Regressions

on Independent Slopes Model (PRISM) maps (Daly *et al.*, 1994), and vegetation-based rainfall estimates to improve the accuracy of the mean rainfall maps. The new Rainfall Atlas of Hawai'i gives only the 30-year mean spatial patterns and does not provide any information about year-to-year rainfall variability. To allow assessment of all types of rainfall variability, including trends, individual month-year maps are needed. However, these maps cannot be produced in the same manner as the mean maps because the predictor variables (vegetation, PRISM, MM5, and radar rainfall maps) do not exist at a monthly temporal resolution over an extended historical period. Therefore, another method is needed to take advantage of the information from the mean Rainfall Atlas maps combined with individual monthly rain gauge totals.

One approach to incorporate long-term mean climatological information with month-year data is to analyse the monthly rainfall anomaly patterns in an approach known as climatologically aided interpolation (CAI) (Willmott and Robeson, 1995). The departures from the mean (anomalies) in a given month-year are interpolated and then combined with the mean map to produce the final month-year map (Dawdy and Langbein, 1960; Peck and Brown, 1962; Jones, 1994; Willmott and Robeson, 1995). This method produces better results than interpolating the raw rainfall totals at a regional scale (New *et al.*, 2000; Chen *et al.*, 2002) and has been used in a number of studies (Dawdy and Langbein, 1960; Peck and Brown, 1962; de Montmollin *et al.*, 1980; Bradley *et al.*, 1987; Willmott and Robeson, 1995; Dai *et al.*, 1997; Brown and Comrie, 2002;

* Correspondence to: A. G. Frazier, Department of Geography, University of Hawai'i at Mānoa, Saunders Hall 418, Honolulu, HI 96822, USA. E-mail: abbyf@hawaii.edu

Mitchell and Jones, 2005; Haylock *et al.*, 2008). It can recreate the climatological pattern even when some of the data are missing for a particular month (Yatagai *et al.*, 2008) because monthly anomalies are likely to be associated with variations in large-scale circulation (New *et al.*, 1999). The majority of studies calculate either the absolute anomaly (individual value minus the mean) or relative anomaly (individual value divided by the mean). Adopting an anomaly approach is appealing for this study because it allows for the spatial information derived from multiple predictor data sets, that were utilized in creating the Rainfall Atlas of Hawai'i maps, to be incorporated in the month-year maps. For precipitation, relative anomalies are preferred over absolute anomalies because the percentage better preserves the relationship between the variance and the mean (New *et al.*, 2000).

Many different geostatistical methods are available for spatially interpolating the anomalies. However, no consensus exists in the literature about which method is best for interpolating monthly rainfall anomalies in complex terrain. One of the most widely used geostatistical interpolation schemes is kriging, which takes advantage of the spatially dependent correlation of environmental variables, assigning more weight to stations nearby (Webster and Oliver, 2007). Kriging also provides an uncertainty estimate, and it is able to easily incorporate secondary variables. In the case of rainfall interpolation, secondary variables include factors such as elevation (Goovaerts, 2000; Mair and Fares, 2011), radar rainfall estimates (Seo *et al.*, 1990; Haberlandt, 2007), and atmospheric variables such as cold cloud duration remotely sensed data (Moges *et al.*, 2007), wind speed, and humidity (Kyriakidis *et al.*, 2001). There are many method variations under the kriging approach, creating a large number of possible combinations when all of the possible covariates combined with the different kriging algorithms are considered.

Previous method evaluations dealt with small station networks and were located in areas with limited terrain variation when compared to Hawai'i (Goovaerts, 2000; Vicente-Serrano *et al.*, 2003; Moral, 2009). This is an important distinction because station network density influences how well the interpolation performs, and landscape heterogeneity has a significant impact on precipitation patterns. Some studies dealt with interpolation on a global scale (New *et al.*, 2000; Chen *et al.*, 2002), which is generally done at a relatively coarse spatial resolution. Many of the studies considered other climate variables such as temperature and soil variables (Bourennane and King, 2003; Hengl *et al.*, 2007), while another common group of results were shown only for daily or hourly rainfall data (Haberlandt, 2007; Yatagai *et al.*, 2008; Haylock *et al.*, 2008). None of these results are directly indicative of which methods will be most successful for interpolating monthly rainfall anomaly data in an area like Hawai'i.

The objective of this study was to create a data set of month-year rainfall maps for the seven major islands of Hawai'i from 1920 to 2012, and to determine the best method for interpolating spatial patterns of relative rainfall anomalies for individual months. For uniformity, it was

desirable to select only one interpolation method to produce the anomaly maps for all islands: the method that performed the best overall. However, the option of using two or more methods was considered if, for example, one method performed significantly better on one island and poorly on the rest of the islands. In the following section, the study domain and available data are described. Details about the different kriging methods, the cross-validation tests used to compare methods, and the procedure for generating the final maps are presented in Section 3. In Section 4, the results of the method comparison are presented along with the examples of the month-year rainfall maps generated for this study. The final section summarizes the findings and presents the discussion and conclusions drawn from this study, as well as suggestions for future research opportunities.

2. Study area and data

2.1. Hawai'i

The area under consideration is the State of Hawai'i, more specifically – the seven major islands Kaua'i, O'ahu, Moloka'i, Lāna'i, Maui, Kaho'olawe, and Hawai'i. The island of Ni'ihau was not considered in this study because no rainfall data were available. The main islands of Hawai'i are located in the Pacific Ocean between 18.9° and 22.24°N latitude, and 160.25° and 154.8°W longitude. The islands have a total land area of 16 637 km² (Juvik and Juvik, 1998), with Hawai'i Island (commonly referred to as the Big Island) comprising 63% of the total.

The climate of the Hawaiian Islands contains a great deal of diversity in a very small area; mean annual rainfall ranges from 204 to 10 271 mm (Giambelluca *et al.*, 2013). This is mainly due to the complex topography and large elevation range (0–4205 m). The average rainfall gradients for some places in Hawai'i are among the steepest in the world, producing a greater range on one small island than generally occurs across an entire continent (Giambelluca *et al.*, 1986). The majority of the rainfall in Hawai'i is produced through orographic lifting as trade winds (east-northeast winds) encounter the windward mountain slopes, producing fairly consistent rainfall patterns throughout the year on these slopes (Giambelluca *et al.*, 2013). At high elevations, however, the growth of clouds is persistently capped by the TWI at about 2200 m (Cao *et al.*, 2007), resulting in steep declines in rainfall above this level.

2.2. Rain gauge database

Over 2000 rain gauge stations have operated across the islands over the past 150 years (Giambelluca *et al.*, 2013), providing an extensive monthly rainfall database. Figure 1 shows the spatial distribution of stations in Hawai'i. The oldest rain gauge in the data set has readings from 1837, and by the year 1968 there were over 950 stations operating at once. However, many stations were discontinued throughout the 1970s and 1980s, and as of 2012, only

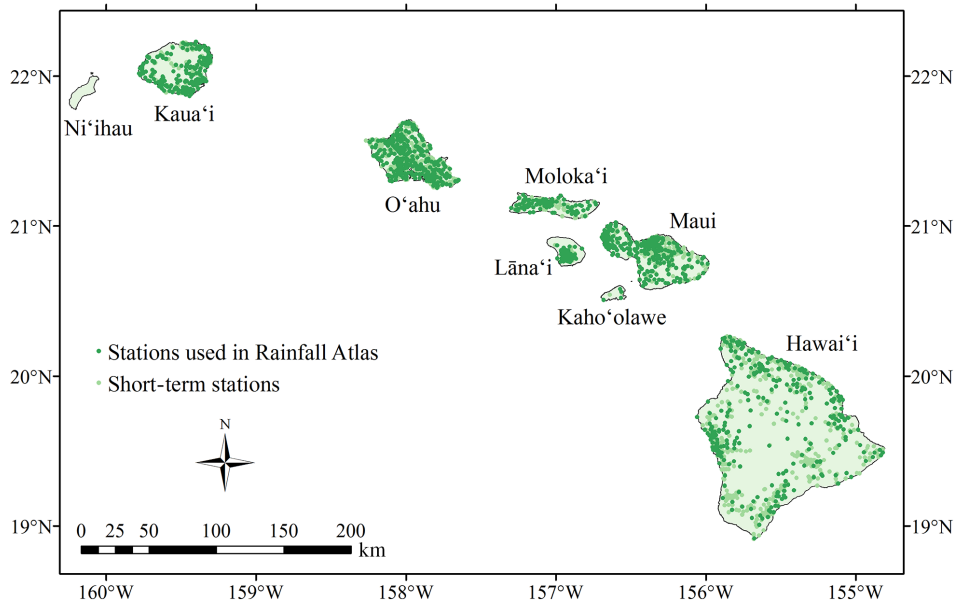


Figure 1. Map of the rain gauge stations in the State of Hawai'i.

404 gauges were still in operation. Many of the discontinued gauges were concentrated in now defunct pineapple and sugarcane plantations, mostly located in low-lying, dry areas of the state. In those areas, the gauge density during the plantation era was greater than that needed to adequately capture the rainfall gradients. Therefore, some of the decline in the number of gauges statewide reduced redundancy in the network.

Data collection was completed in two rounds: the first collected all data from 1920 to 2007, and the second from 2008 to 2012. The data were collected from various sources, the largest being a database maintained by the Hawai'i Department of Land and Natural Resources and the Office of the State Climatologist. Monthly rainfall data were also collected from the National Climatic Data Center (NCDC), the U.S. Geological Survey (USGS), and several small networks including HaleNet (Haleakalā Climate Network, operated by the Geography Department at the University of Hawai'i at Mānoa), HydroNet (operated by the National Weather Service), and RAWS (Remote Automated Weather Stations, data available through the Western Regional Climate Center, WRCC). After the data were compiled, a variety of gap filling techniques (Paulhus and Kohler, 1952; Eischeid *et al.*, 2000) were performed on the data set to improve the temporal and spatial resolution. Many quality control techniques were used to screen the data, including homogeneity testing using a penalized maximal *t*-test (Wang *et al.*, 2007; Wang, 2008) and manual screening for outliers and suspicious values (Giambelluca *et al.*, 2013).

The 1920–2007 data set contained over 1100 stations, and was used to produce the Rainfall Atlas mean maps. Although the temporal and spatial resolution was greatly improved through gap filling, the station network still varied through time. The rain gauge means over the most recent 30-year period available (1978–2007) were fused

with spatial predictor data sets (PRISM, radar, mesoscale model output, and vegetation-derived rainfall, which were incorporated using virtual rain gauge stations). The result was a set of 12 monthly maps and one annual map of mean rainfall at spatial resolution of 250 m. For the complete database development methods, see Giambelluca *et al.* (2013).

The 2008–2012 data collection added 120 more stations to the full data set, including data from two new sources. However, as mentioned previously, many of the long-term stations had been discontinued which resulted in an overall loss of stations, even after gap filling. On average, across the state there were 185 fewer stations in the 2008–2012 data set. The largest percentages of stations lost were on Lāna'i and Moloka'i, losing 31 stations on average (61%) and 50 stations on average (57%), respectively. For months with low station numbers (less than ten), these two islands were interpolated together as they are located only 15 km apart.

3. Methods

3.1. Kriging methods

The 30-year mean monthly rainfall maps from the Rainfall Atlas of Hawai'i along with the monthly rainfall database served as the two major inputs for creating the month-year maps. The data values at every rain gauge station were converted into dimensionless relative anomalies by dividing the station value by the mean monthly value at that location (e.g. a January data value was divided by the January mean value). To go from a finite number of irregularly spaced points (rain gauge sites) to a high-resolution gridded surface (rainfall map), some form of interpolation is required.

Kriging refers to a subset of geostatistical interpolation methods that rely on the spatial structure of the data,

assuming data points that are closer together are more alike than points that are further apart. Kriging uses a semi-variogram to assess the dissimilarity between points in a search neighbourhood. The experimental semi-variogram $\hat{\gamma}(h)$ at lag h for a set of data $z(x_i)$, $i = 1, 2, \dots$, is shown in Equation (1):

$$\hat{\gamma}(h) = \frac{1}{2N(h)} \sum_{i=1}^{N(h)} [z(x_i) - z(x_i + h)]^2 \quad (1)$$

where $N(h)$ is the number of pairs of data points separated by a vector h . The spherical model, characterized by linear behaviour at the origin with a gradual curve towards the sill (Goovaerts, 2000), is used in this study to model the variograms. The spherical model is the most widely used model because it usually provides the best fit in one-, two-, and three-dimensions. The equation for the spherical model is shown in Equation (2):

$$\gamma(h) = \begin{cases} c \left[\frac{3h}{2a} - \frac{1}{2} \left(\frac{h}{a} \right)^3 \right] & \text{for } h \leq a \\ c & \text{for } h > a \end{cases} \quad (2)$$

where c is the sill variance and a is the range (Webster and Oliver, 2007).

Kriging is an unbiased and optimal estimator, where the weights used for the points must sum to one, and the goal of the estimator is to minimize the estimation variance (Goovaerts, 1997). Kriging estimates values of a variable Z given known values $z(x_1)$, $z(x_2)$, \dots , $z(x_N)$, at points x_1 , x_2 , \dots , x_N . Ordinary kriging (OK) is the most frequently used and robust type of kriging. Equation (3) shows the OK estimator, to estimate Z at a point x_0 :

$$\hat{Z}(x_0) = \sum_{i=1}^N \lambda_i z(x_i) \quad (3)$$

where λ_i are the weights. OK interpolates the point data alone (without secondary variables), and solves a system of $N + 1$ equations with $N + 1$ unknowns to determine the weights that minimize the estimation variance. OK is used in most method comparison studies as a base method against which to compare other methods (Goovaerts, 2000; Kyriakidis *et al.*, 2001; Moges *et al.*, 2007; Moral, 2009; Mair and Fares, 2011; Sanchez-Moreno *et al.*, 2014). In most of these studies, methods that incorporate a secondary variable proved to outperform OK. However, Mair and Fares (2011) found in their study on west O'ahu island, Hawai'i, that OK consistently performed the best, and Sanchez-Moreno *et al.* (2014) found that OK produced the best cross-validation results on Santiago Island, Cape Verde.

Ordinary cokriging (OCK) is one of many kriging methods that incorporate a secondary variable. OCK capitalizes on the cross-semivariance between the primary and secondary variables, and incorporates that information into the kriging matrix. This makes OCK more computationally expensive and complex than OK. For one secondary

variable y , the OCK estimator is shown in Equation (4):

$$\hat{Z}(x_0) = \sum_{i_1=1}^{N_1} \lambda_{i_1} z(x_{i_1}) + \sum_{i_2=1}^{N_2} \lambda'_{i_2} z(x'_{i_2}) \quad (4)$$

where the weights (λ_{i_1}) are for the N_1 z samples, and the weights (λ'_{i_2}) are for the N_2 y samples. For OCK, the weights are constrained such that the sum of the weights for the primary variable (λ_{i_1}) must equal one, and the weights for the secondary variable (λ'_{i_2}) must sum to zero.

Another way to include secondary information is in the form of an external drift or trend, as in the kriging with external drift method (KED). Unlike OK which uses a constant (unknown) mean, KED can account for non-stationarity in the mean across the study area because the linear relationship between the external variable(s) and the rainfall is assessed locally (Goovaerts, 2000). This method requires the external variable to vary smoothly in space and to be known at every location to be estimated. It also assumes a linear relationship between the target variable and drift variable (Deutsch and Journel, 1998; Bourennane and King, 2003; Webster and Oliver, 2007). With KED, both the deterministic and stochastic components are fitted simultaneously so that the drift variable is incorporated into the kriging system (Webster and Oliver, 2007). KED with one external variable uses $N + 2$ equations to solve for the weights, accounting for the two constraints on the weights. The KED estimator is shown in Equation (5):

$$\hat{Z}_{\text{KED}}(x_0) = \sum_{i=1}^N \lambda_i^{\text{KED}} z(x_i) \quad (5)$$

This method was chosen because it has been shown to outperform OK and OCK (Goovaerts, 2000; Kyriakidis *et al.*, 2001; Moral, 2009).

All kriging methods assume that the data are normally distributed. Precipitation data, however, are often positively skewed, which results in semivariances that are less reliable (Webster and Oliver, 2007). In Hawai'i, the distributions of relative anomalies varied for every island-month, where some were close to normal while others were skewed. The common solution of transforming the data can improve the interpolation error (Tait *et al.*, 2006; Erdin *et al.*, 2012; Song *et al.*, 2015). To assess the effect of transforming relative anomaly data before kriging, two common transformations (square root and log) were used on a sample of island-months with positively skewed distributions. Both the transformed and original data were interpolated and the performances were compared using cross-validation (see Section 3.3). Neither transformation improved the results significantly, a result similar to that of Erdin *et al.* (2012) who found only small differences in the point estimates between KED with and without transformation. Therefore, all kriging interpolations were performed on original, un-transformed data.

3.2. Secondary variables

In many studies, a secondary variable is shown to greatly improve interpolation results (Goovaerts, 2000; Kyriakidis

et al., 2001; Moges *et al.*, 2007; Moral, 2009). A densely sampled or spatially continuous secondary variable can improve the measurement of the primary variable that may be less densely sampled, because it draws from existing patterns rather than the stations alone. The first variable considered as a covariate for this project was elevation. Elevation has been used by many to help interpolate rainfall because of the strong orographic influences on precipitation (Daly *et al.*, 1994). Sanchez-Moreno *et al.* (2014) found that elevation explained most of the variance in rainfall, particularly for low and medium rainfall events that were likely orographic in origin. However, other studies have shown that when compared with atmospheric variables, elevation is not very well correlated with rainfall data (Kyriakidis *et al.*, 2001). Because it is one of the most commonly used covariates and given the importance of orographic lifting in Hawai'i, elevation was included as one of the secondary variables tested. A 30 m resolution digital elevation model (DEM) of the state was used for the elevation input. The other variable used as a covariate was mean monthly rainfall from the 2013 Rainfall Atlas (250 m resolution raster maps, Giambelluca *et al.*, 2013). Some studies have found that mean rainfall surfaces were much better predictors than elevation (Daly *et al.*, 2004; Tait *et al.*, 2006). These mean maps contain additional information about the complex rainfall patterns through the incorporation of predictor data sets (i.e. PRISM and MM5). Therefore, other possible covariates such as latitude, longitude, slope, and aspect were not considered in this study.

3.3. Method comparison

For the method comparison, each calendar month was tested on each island for a 30-year period. The number of gauges varied throughout time as the station network evolved, and the period 1940–1969 was chosen for the comparison because it had the highest numbers of stations in operation within the full study period. For the method comparison and mapping, Kaho'olawe, with only five stations, was combined with Maui. The other five islands were analysed independently.

ArcGIS™ 10 (ESRI, 2011; Redlands, CA, USA) was the main software package used to conduct the method comparison, as OK and OCK methods were available in the program. Because ArcGIS™ also gave the option to auto-fit variogram parameters and has a more powerful user interface than R (R Core Team, 2014) to visualize and prepare final maps (Hengl *et al.*, 2007), it was used as the primary program for producing OK and OCK maps, and for processing the final maps. KED is not available in ArcGIS™ 10 and, therefore, another geostatistical software package, GSLIB (Deutsch and Journel, 1998), was used. Unlike ArcGIS™, GSLIB requires the user to develop variogram models manually. Kriging methods were run for all islands from 1940 to 1969 for each month, with unique variograms fit for each month-year, and cross-validation outputs were saved.

The kriging methods were assessed by comparing the cross-validation statistics for the different methods. The

cross-validation process sequentially withholds a point and uses the remaining data to predict its value, and then compares the predicted and measured values. While some weaknesses with this technique have been shown (Jeffrey *et al.*, 2001), it is the most widely used approach for method intercomparisons. The mean absolute error (MAE) and the root mean square error (RMSE) were used to assess and compare the methods (Willmott, 1982). Both MAE and RMSE express errors in the same units as the rainfall. MAE is a measure of average error, and RMSE is a measure of random error (scatter). The MAE and RMSE equations are shown in Equations (6) and (7):

$$\text{MAE} = \frac{1}{N} \sum_{i=1}^N |p_i - o_i| \quad (6)$$

$$\text{RMSE} = \left[\frac{1}{N} \sum_{i=1}^N (p_i - o_i)^2 \right]^{1/2} \quad (7)$$

where N is the count of stations, p_i are the predicted values at each station, and o_i are the observed values. The MAE and RMSE values for each station were computed for every island-month and year for all five methods: OK, OCK with elevation, OCK with mean rainfall, KED with elevation, and KED with mean monthly rainfall.

A ranking system was developed to choose the best method for each island-month, incorporating the performance evaluations based on the cross-validation statistics. For every island-month, the five methods were ranked 1–5 (best to worst) based on four different criteria: lowest mean MAE value, highest percentage of years (out of 30) with the lowest MAE value, lowest mean RMSE value, and highest percentage of years (out of 30) with the lowest RMSE value. The method with the lowest average rank across the four categories was deemed the best method for that island-month (Hofstra *et al.*, 2008). For any islands where a single method did not prevail as the best in all months, single factor analysis of variance (ANOVA) was used to compare the mean statistics for all five methods to test for statistically significant differences between method performances ($\alpha = 0.05$). To assess the impact of CAI (interpolating anomalies instead of original rainfall data) on the method comparison results, the original month-year rainfall values were interpolated directly for comparison. This test was performed for a 10-year sample for 2 months on one island, and the cross-validation statistics were compared.

3.4. Final maps

To produce the final month-year rainfall maps, relative anomalies were interpolated for the remaining month-years that had not already been completed in the method comparison step, i.e. before and after 1940–1969, using the 'best' method determined from the method comparison. To ensure that the auto-fit variogram parameters produced reasonable patterns, all geostatistical layers and fitted variogram models were examined manually. The month-year anomaly maps were saved with the same

Table 1. Minimum, maximum, and mean number of rain gauge stations used to make the maps for each island (over all months, 1920–2012), as well as land area (km²) of each island (Juvik and Juvik, 1998) and minimum, maximum, and mean station densities (gauges per km²).

	Minimum number gauges	Maximum number gauges	Mean number gauges	Area (km ²)	Minimum station density	Maximum station density	Mean station density
Kaua'i	111	211	178	1430.5	0.078	0.148	0.124
O'ahu	250	356	309	1546.5	0.162	0.230	0.200
Moloka'i	14	87	69	673.5	0.021	0.129	0.102
Lāna'i	1	50	42	364.0	0.003	0.137	0.115
Maui	198	264	233	1999.2	0.099	0.132	0.117
Hawai'i	255	348	302	10433.1	0.024	0.033	0.029

Maui values includes the island of Kaho'olawe.

Table 2. Best interpolation method for each island-month based on the lowest average rank from cross-validation test, 1940–1969.

	Hawai'i	Kaua'i	Lāna'i	Maui	Moloka'i	O'ahu
January	OK	OK	OK	OCK_RF	OK	OK
February	OK	OK	OK	OCK_RF	OCK_RF	OK
March	OK	OK	KED_RF	OK	OCK_RF	OK
April	OK	OK	KED_RF	OK	OCK_RF	OK
May	OK	OK	OK	OK	OCK_RF	OK
June	OK	OK	KED_RF	OCK_RF	OK	OK
July	OK	OK	OCK_RF	OK	OCK_RF	OK
August	OK	OK	OK	OK	OK	OK
September	OK	OK	OK	OK	OK	OK
October	OK	OK	OK	OK	OK	OK
November	OK	OK	OCK_RF	OK	OCK_RF	OK
December	OK	OK	KED_RF	OCK_RF	OCK_RF	OK

OK, ordinary kriging; KED_RF, kriging with external drift with mean rainfall; OCK_RF, ordinary cokriging with mean rainfall.

extent and 250 m spatial resolution as the Rainfall Atlas mean maps. The anomaly maps were multiplied by the Rainfall Atlas of Hawai'i mean monthly maps to produce the final month-year rainfall maps (e.g. January anomaly maps were multiplied by the January mean map). The 12 monthly maps in each year were then summed to produce annual maps for each year. Table 1 documents the minimum, maximum, and mean number of rain gauge stations used on each island, as well as station densities.

4. Results

4.1. Method comparison

Table 2 shows the best interpolation methods chosen by each island-month based on the MAE and RMSE values using the ranking procedure described in the previous section. Based on these results, OK was chosen as the best method to use for interpolating rainfall anomalies in Hawai'i. Overall, OK showed the smallest cross-validation errors (had the least bias and scatter) compared to the other four methods, and outperformed the other methods for 55 of the total 72 island-months (Table 2). This result was unequivocal in three of the islands (Kaua'i, O'ahu, and Hawai'i islands), while for the other islands OK was selected for about half of the months. For the 17 island-months where OK was not chosen as the best method, the ANOVA results indicated that the OK method was not statistically significantly different from the method identified as the best. Therefore, because OK performed

well in these island-months despite not having the best ranked statistics, OK was selected as the method used to interpolate the anomalies for all island-months. An example of the differences in the rainfall surfaces produced by the five methods is shown in Figure 2 for 1 month-year for O'ahu (May 1964), a month where OK had the lowest cross-validation statistics of all five methods. For this particular month-year, the spatial patterns are very similar for all five methods; however, OK predicts less rainfall in the peak areas compared to the other methods (particularly KED). The overall cross-validation results (scatter plots of predicted versus measured values) for O'ahu in May are shown for the five methods in Figure 3, an example island-month where OK outperformed the other methods. When original rainfall data were interpolated (instead of anomalies) for the sample island-months, no significant difference was found in the performance between OK and the methods including a secondary variable.

4.2. Final maps

A total of 7254 anomaly maps and 7254 rainfall maps were created. To illustrate the results, Figure 4 shows an example time series of rainfall maps for 10 years in December on Hawai'i Island, while Figure 5 displays the corresponding anomaly maps. All month-year maps are available as raster GIS (Geographic Information Systems) layers and can be downloaded from the Rainfall Atlas website: <http://rainfall.geography.hawaii.edu/downloads.html>. The mean monthly rainfall statistics

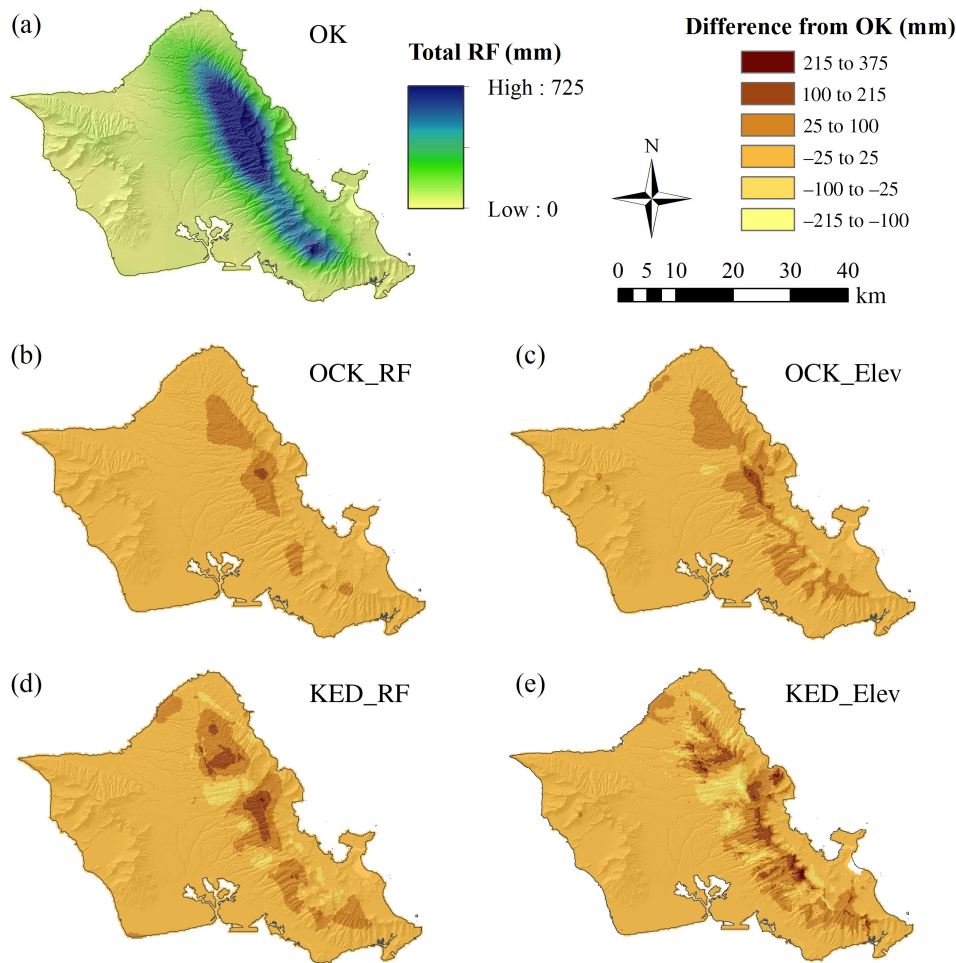


Figure 2. Comparison of five method outputs for O'ahu Island, May 1964 rainfall (in millimetres). (a) Predicted rainfall surface produced by ordinary kriging (OK) with a rainfall range of 0–725 mm. (b–e) Difference in predicted rainfall for the other four methods from the OK surface. (b) Ordinary cokriging with mean rainfall as a covariate minus OK, (c) ordinary cokriging with elevation as a covariate minus OK, (d) kriging with external drift using mean rainfall as a covariate minus OK, and (e) kriging with external drift using elevation as a covariate minus OK.

are shown in Figure 6 for each island, where the typical annual cycle is apparent: dry season during summer months and wet season in winter months.

5. Discussion and conclusions

Month-year rainfall maps of the major Hawaiian Islands were produced from 1920 to 2012 using OK of the relative rainfall station anomalies. A secondary variable was not shown to improve the interpolation, a result contrary to many previous studies (Goovaerts, 2000; Kyriakidis *et al.*, 2001; Moges *et al.*, 2007). However, none of these other studies were performed for a terrain comparable to Hawai'i, or with a similar station network density (Table 3). The only previous study that fully corroborates these results was that of Mair and Fares (2011), who found that over a small area on western O'ahu, OK produced more accurate rainfall predictions than simple kriging with varying local means (SKlm), using elevation and distance to a regional rainfall maximum as the two secondary variables; SKlm has been shown to produce results similar to KED, the method used in this study (Goovaerts, 2000).

The fact that OK produces better results in Hawai'i than methods incorporating secondary variables, such as KED and SKlm, is most likely due to the extremely high rain gauge density in Hawai'i. The Mair and Fares (2011) study used 21 gauges over a 280 km² area (0.082 gauges km⁻²). As seen in Table 1, mean station densities on all islands (except Hawai'i Island) in this study exceed that value, ranging from 0.102 gauges km⁻² on Moloka'i to 0.200 gauges km⁻² on O'ahu (0.029 gauges km⁻² on Hawai'i Island). These values are considerably higher than all previous studies examined (Table 3). The main purpose of incorporating a secondary variable is to add information not represented in the primary variable, thereby increasing precision. However, this added information will only improve the precision of the interpolation if the primary variable is severely under-sampled (e.g. low rain gauge station density).

Another reason why a secondary variable did not improve the prediction surface could be that most of the information about the surface was already incorporated by interpolating anomalies instead of raw rainfall values. The mean rainfall maps used to create the anomalies contain

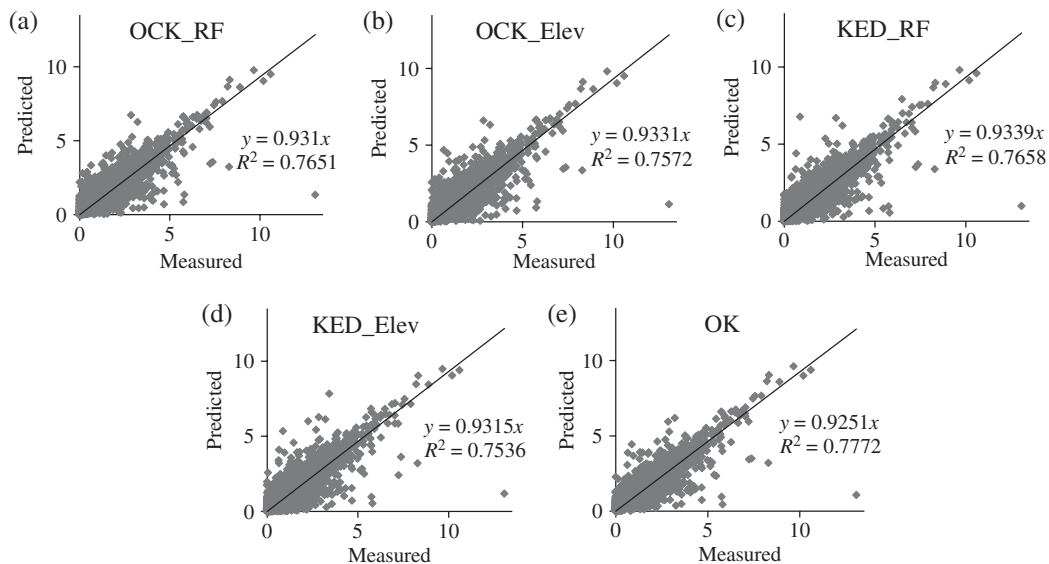


Figure 3. O’ahu Island cross-validation results for the month of May from 1940 to 1969 for the five methods tested. (a) Scatter plot of measured *versus* predicted rainfall for ordinary cokriging with mean rainfall as a covariate, (b) measured *versus* predicted values from ordinary cokriging with elevation as a covariate, (c) measured *versus* predicted values from kriging with external drift using mean rainfall as a covariate, (d) measured *versus* predicted values from kriging with external drift using elevation as a covariate, and (e) the scatter plot of measured *versus* predicted rainfall for ordinary kriging.

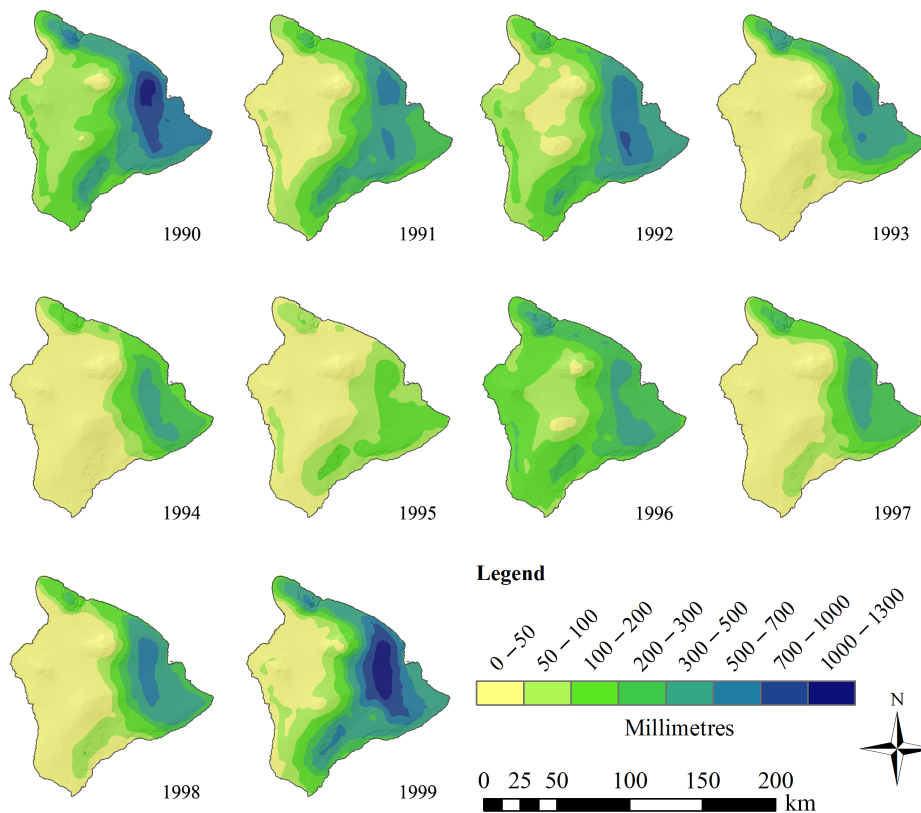


Figure 4. Ten-year time series of December rainfall maps for Hawai’i Island from 1990 to 1999.

additional information that was not available at a monthly time scale. If this test were to be performed with a monthly time series of covariates (such as monthly wind speed or humidity), instead of with a variable that is fixed in time, we might expect better cross-validation results than those produced by OK. Unfortunately, variables such as

humidity and wind, that have been shown to outperform elevation as secondary variable used to interpolate precipitation (Kyriakidis *et al.*, 2001), are not available in gridded month-year format for Hawai’i. Possible improvements in the predicted surface by using one of these other variables would be most important in areas where the rain gauge

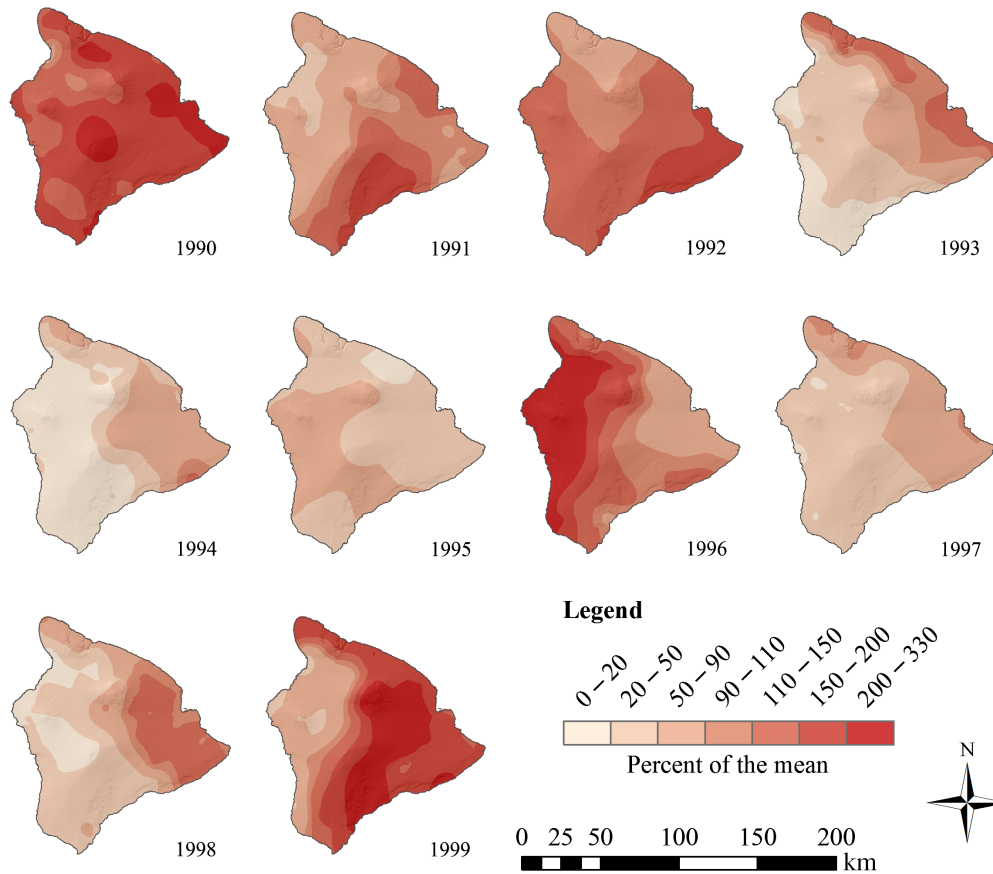


Figure 5. Ten-year time series of December relative anomaly (estimated value divided by climatology) maps for Hawai'i Island from 1990 to 1999.

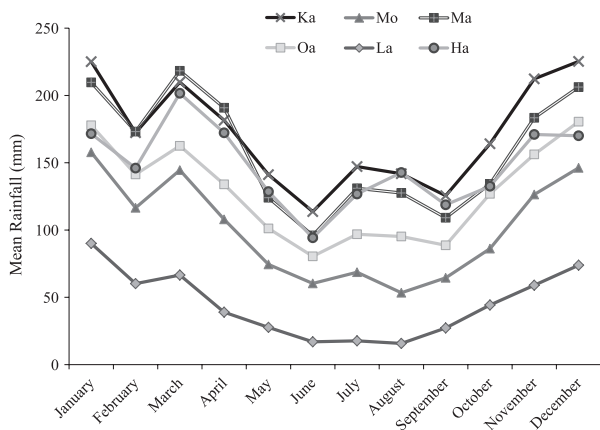


Figure 6. Mean monthly rainfall statistics derived from the month-year maps, averaged over all 93 years (in mm) for each island-month. Ka is Kauai, Oa is Oahu, Mo is Molokai, La is Lana'i, Ma is Maui, and Ha is Hawaii Island.

network is sparse, particularly on Hawai'i Island, where station densities are the lowest. However, because no significant difference between the methods was seen when original rainfall values (instead of anomalies) were interpolated, this indicates that the likely reason OK performed better is not due to additional information gained through CAI, but rather due to high station density.

Although OK was the best method for the majority of island-months (Table 2), other methods performed

marginally better in a few instances. OCK with mean rainfall as a covariate (OCK_RF) had the best cross-validation statistics for 13 of the 17 island-months where OK was not the best method. Use of elevation as a covariate did not produce the best results for any island-month. OCK_RF performed best on Molokai Island in particular (7 of 12 months). This island had the highest number of virtual stations used in the mean Rainfall Atlas map to fill spatial gaps in the gauge network, and has very steep rainfall gradients that are difficult to interpolate. Therefore, it would make sense that the additional information from the mean map could improve the prediction.

These month-year maps reveal extreme month-to-month variation in the spatial patterns of rainfall. Figures 4 and 5 show an example 10-year time series of maps from 1990 to 1999 for December on Hawai'i Island and the corresponding anomaly maps. The extreme range in values that can occur on a single island is also apparent in these figures, where, for example, December 1999 on Hawai'i Island had some areas with less than 20 mm, while other areas received almost 1300 mm in that month-year (Figure 4). The spatial patterns can also vary significantly from year-to-year, which can be seen clearly in the anomalies in Figure 5. December 1996 shows the western half of the island with over 200% of the mean December values, while December 1990 shows high anomalies distributed almost evenly across the island.

Table 3. Previous geostatistical interpolation studies with study area, number of rain gauges used, land area, and gauge station density (gauges per km²).

Study	Location	Number of gauges	Area (km ²)	Station density
Brown and Comrie, 2002	Southwest USA	572	1 395 000 ^a	0.0004
Goovaerts, 2000	Algarve, Portugal	36	5000	0.0072
Haberlandt, 2007	Elbe basin, Germany	302	25 000	0.0121
Haylock <i>et al.</i> , 2008	All of Europe	2316	10 000 000 ^a	0.0002
Kyriakidis <i>et al.</i> , 2001	Northern CA, USA	77	108 000	0.0007
Mair and Fares, 2011	West O'ahu, HI, USA	23	280	0.0821
Moges <i>et al.</i> , 2007	Rufuji basin, Tanzania	704	177 000	0.0040
Moral, 2009	Extremadura, Spain	136	41 600	0.0033
Sanchez-Moreno <i>et al.</i> , 2014	Santiago Island, Cape Verde	27	991	0.0272
Vicente-Serrano <i>et al.</i> , 2003	Ebro Valley, Spain	380	20 000 ^a	0.0190

^aApproximate value.

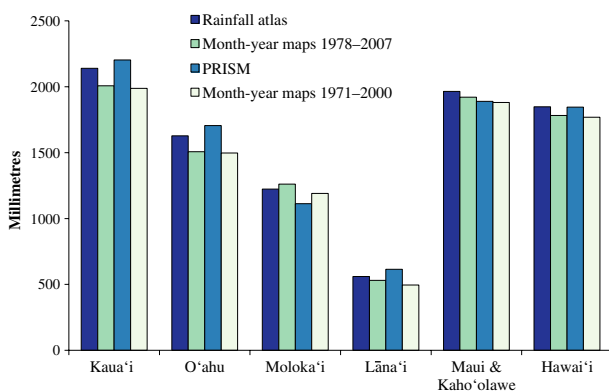


Figure 7. Comparison of mean annual rainfall values (in millimetres) between the updated Rainfall Atlas (base period 1978–2007), PRISM maps (base period 1971–2000), and the 30-year mean values from the month-year maps (this study) to match these two base periods.

As a consistency check on the new maps, a 30-year climatological mean value was calculated for each island from the month-year maps and compared with the existing 30-year mean maps. Figure 7 shows this comparison between the calculated annual mean from the month-year maps, the 2013 Rainfall Atlas annual maps (average of the 1978–2007 rainfall), and the 1971–2000 PRISM maps (Daly *et al.*, 2006) for each island. The month-year map means were calculated for each of the separate base periods used in the Rainfall Atlas and PRISM maps. When the means were compared, the month-year annual estimate showed an underestimation of the mean for all islands (except Moloka'i, where the month-year map means were greater). Kaua'i and O'ahu showed the largest discrepancies, where the month-year maps averaged about 170 mm lower. One reason could be that these other climatologies include more information (such as vegetation information), that was not available at the monthly scale to use in this project. Without complete spatial rain gauge coverage or accurate satellite data, it is impossible to interpolate with perfect accuracy. All of these maps, including the Rainfall Atlas and PRISM climatologies, are best approximations with the information available.

This study provides a template for generating current month-year rainfall maps as new data become available.

Because of the reduced size of the current station network, gap filling should be applied to take advantage of the rich information provided by historical stations and reduce error in the interpolation, as variability in the station network through time can affect the smoothness of the interpolated surfaces. Figure S1, Supporting Information, shows the time series of average annual RMSE results for the state from 1920 to 2012 and the scatter plot relating the RMSE values with the average number of stations in each year. The time series shows a slight increasing trend in RMSE over time, likely related to the overall station network declines over this period. The scatter plot shows the expected negative relationship, indicating higher error when fewer stations were operating. Although gap filling can help to reduce this error, the success of gap filling attempts depends on the availability of sufficient stations to establish robust statistical relationships. This was the case for Lāna'i when the 2008–2012 data were added to the data set; only seven stations were operating intermittently during this time, which made it difficult to gap fill historical stations in all months. A better solution would be to install more rain gauges across the state. Table 1 shows the bias in station placement, where the island of O'ahu has about the same number of stations as Hawai'i island, which is six times the size of O'ahu. Installation of new gauges should take into account the locations of current stations and long-term stations that have been discontinued (to possibly continue these records), as well as where the largest spatial gaps are found. In particular, the islands of Lāna'i, Moloka'i, and Hawai'i should be prioritized, as these islands have the lowest minimum station densities (Table 1).

In summary, month-year rainfall maps from 1920 to 2012 have been generated for Hawai'i, with accompanying anomaly maps relative to the 1978–2007 mean. Based on cross-validation results, OK was found to outperform OCK and KED using elevation and mean rainfall as secondary variables. The final maps were created by using OK to interpolate the anomaly values, and then combining the anomaly surfaces with the mean maps. This procedure can be used in the future to produce near real time month-year maps as the data become available.

Acknowledgements

The authors thank Dr Matthew McGranaghan and Dr Qi Chen for their geostatistical advice, and Dr Ryan Longman for his continuous support. This project was made possible through funding developed under an agreement between the State of Hawai'i Commission on Water Resource Management and the U.S. Army Corps of Engineers, Honolulu District, under Section 22 of the Water Resources Development Act of 1974. This research was also partially supported by the USGS Pacific Islands Water Science Center and a grant from the National Oceanic and Atmospheric Administration's (NOAA) Climate Program Office under its Climate Change and Data Detection program (award number NA09OAR4310103), and by the Pacific Islands Climate Change Cooperative (PICCC) award F10AC00077.

Supporting Information

The following supporting information is available as part of the online article:

Figure S1. Time series of average annual root mean square error (RMSE) results for the State of Hawai'i and scatter plot of RMSE versus average number of stations (1920–2012).

References

- Bourennane H, King D. 2003. Using multiple external drifts to estimate a soil variable. *Geoderma* **114**: 1–18.
- Bradley RS, Diaz HF, Eischeid JK, Jones PD, Kelly PM, Goodness CM. 1987. Precipitation fluctuations over Northern Hemisphere land areas since the mid-19th century. *Science* **237**: 171–175.
- Brown DP, Comrie AC. 2002. Spatial modeling of winter temperature and precipitation in Arizona and New Mexico, USA. *Clim. Res.* **22**: 115–128.
- Cao G, Giambelluca TW, Stevens DE, Schroeder TA. 2007. Inversion variability in the Hawaiian trade wind regime. *J. Clim.* **20**: 1145–1160, doi: 10.1175/JCLI4033.1.
- Chen M, Xie P, Janowiak JE, Arkin PA. 2002. Global land precipitation: a 50-yr monthly analysis based on gauge observations. *J. Hydrometeorol.* **3**: 249–266.
- Dai A, Fung IY, Del Genio AD. 1997. Surface observed global land precipitation variations during 1900–88. *J. Clim.* **10**: 2943–2962.
- Daly C, Neilson RP, Phillips DL. 1994. A statistical-topographic model for mapping climatological precipitation over mountainous terrain. *J. Appl. Meteorol.* **33**: 140–158.
- Daly C, Gibson W, Doggett M, Smith J, Taylor G. 2004. Up-to-date monthly climate maps for the conterminous United States. In *Proceedings of the 14th AMS Conference on Applied Climatology*, American Meteorological Society, Seattle, WA, January 13–16, 2004, P 5.1.
- Daly C, Smith J, Doggett M, Malbleib M, Gibson W. 2006. High-resolution climate maps for the Pacific Basin Islands, 1971–2000. Report submitted to National Park Service Pacific West Regional Office. PRISM Group, Oregon State University.
- Dawdy DR, Langbein WB. 1960. Mapping mean areal precipitation. *J. Hydrol. Sci. J.* **5**: 16–23.
- Deutsch CV, Journel AG. 1998. *GSLIB, Geostatistical Software Library and User's Guide*, 2nd edn. Oxford University Press: New York, 368 pp.
- Eischeid JK, Pasteris PA, Diaz HF, Plantico MS, Lott NJ. 2000. Creating a serially complete, national daily time series of temperature and precipitation for the western United States. *J. Appl. Meteorol.* **39**: 1580–1591.
- Erdin R, Frei C, Kunsch HR. 2012. Data transformation and uncertainty in geostatistical combination of radar and rain gauges. *J. Hydrometeorol.* **13**: 1332–1346.
- ESRI. 2011. *ArcGIS Desktop: Release 10*. Environmental Systems Research Institute: Redlands, CA.
- Giambelluca TW, Nullet MA, Schroeder TA. 1986. *Rainfall Atlas of Hawai'i*. Department of Land and Natural Resources, University of Hawai'i at Mānoa: Honolulu, HI.
- Giambelluca TW, Chen Q, Frazier AG, Price JP, Chen Y-L, Chu P-S, Eischeid JK, Delparte DM. 2013. Online rainfall atlas of Hawai'i. *Bull. Am. Meteorol. Soc.* **94**: 313–316, doi: 10.1175/BAMS-D-11-00228.1.
- Goovaerts P. 1997. *Geostatistics for Natural Resources Evaluation*. Oxford University Press: New York, NY, 483 pp.
- Goovaerts P. 2000. Geostatistical approaches for incorporating elevation into the spatial interpolation of rainfall. *J. Hydrol.* **228**: 113–129.
- Haberlandt U. 2007. Geostatistical Interpolation of hourly precipitation from rain gauges and radar for a large-scale extreme rainfall event. *J. Hydrol.* **332**: 144–157, doi: 10.1016/j.jhydrol.2006.06.028.
- Haylock MR, Hofstra N, Klein Tank AM, Klok EJ, Jones P, New M. 2008. A European daily high-resolution gridded dataset of surface temperature and precipitation for 1950–2006. *J. Geophys. Res.* **113**: D20119, doi: 10.1029/2008JD010201.
- Hengl T, Heuvelink GB, Rossiter DG. 2007. About regression-kriging: from equations to case studies. *Comput. Geosci.* **33**: 1301–1315.
- Hofstra N, Haylock M, New M, Jones P, Frei C. 2008. Comparison of six methods for the interpolation of daily, European climate data. *J. Geophys. Res.* **113**(D21110): 1–19, doi: 10.1029/2008JD010100.
- Jeffrey SJ, Carter JO, Moodie KB, Beswick AR. 2001. Using spatial interpolation to construct a comprehensive archive of Australian climate data. *Environ. Model. Softw.* **16**: 309–330.
- Jones PD. 1994. Hemispheric surface air temperature variations: a reanalysis and an update to 1993. *J. Clim.* **7**: 1794–1802.
- Juvik SP, Juvik JO. 1998. *Atlas of Hawai'i*, 3rd edn. University of Hawai'i Press: Honolulu, HI, 333 pp.
- Kyriakidis PC, Kim J, Miller NL. 2001. Geostatistical mapping of precipitation from rain gauge data using atmospheric and terrain characteristics. *J. Appl. Meteorol.* **40**: 1855–1877.
- Mair A, Fares A. 2011. Comparison of rainfall interpolation methods in a mountainous region of a tropical island. *J. Hydrol. Eng.* **16**: 371–383, doi: 10.1061/(ASCE)HE.1943-5584.0000330.
- Mitchell TD, Jones PD. 2005. An improved method of constructing a database of monthly climate observations and associated high-resolution grids. *Int. J. Climatol.* **25**: 693–712.
- Moges SA, Alemaw BF, Chaoka TR, Kachroo RK. 2007. Rainfall interpolation using a remote sensing CCD data in a tropical basin – a GIS and geostatistical application. *Phys. Chem. Earth* **32**: 976–983.
- de Montmollin FA, Oliver RJ, Simard RG, Zwahlen F. 1980. Evaluation of a precipitation map using a smoothed elevation-precipitation relationship and optimal estimates (Kriging). *Nord. Hydrol.* **11**: 113–120.
- Moral FJ. 2009. Comparison of different geostatistical approaches to map climate variables: application to precipitation. *Int. J. Climatol.* **30**: 620–631, doi: 10.1002/joc.1913.
- New M, Hulme M, Jones P. 1999. Representing twentieth-century space-time climate variability. Part I: development of a 1961–90 mean monthly terrestrial climatology. *J. Clim.* **12**: 829–856.
- New M, Hulme M, Jones P. 2000. Representing twentieth-century space-time climate variability. Part II: development of 1901–1996 monthly grids of terrestrial surface climate. *J. Clim.* **13**: 2217–2238.
- Paulhus JL, Kohler MA. 1952. Interpolation of missing precipitation records. *Mon. Weather Rev.* **80**: 129–133.
- Peck EL, Brown MJ. 1962. An approach to the development of isohyetal maps for mountainous areas. *J. Geophys. Res.* **67**: 681–694.
- R Core Team. 2014. *R: A Language and Environment for Statistical Computing*. R Foundation for Statistical Computing: Vienna. <http://www.R-project.org/> (accessed 7 November 2014).
- Sanchez-Moreno JF, Mannaerts CM, Jetten V. 2014. Influence of topography on rainfall variability in Santiago Island, Cape Verde. *Int. J. Climatol.* **34**: 1081–1097.
- Seo DJ, Krajewski WF, Azimi-Zonooz A, Bowles DS. 1990. Stochastic interpolation of rainfall data from rain gauges and radar using cokriging 2. Results. *Water Resour. Res.* **26**: 915–924.
- Song JJ, Kwon S, Lee GW. 2015. Incorporation of parameter uncertainty into spatial interpolation using Bayesian trans-Gaussian kriging. *Adv. Atmos. Sci.* **32**: 413–423.
- Tait A, Henderson R, Turner R, Zheng X. 2006. Thin plate smoothing spline interpolation of daily rainfall for New Zealand using a climatological rainfall surface. *Int. J. Climatol.* **26**: 2097–2115.
- Vicente-Serrano SM, Saz-Sanchez MA, Cuadrat JM. 2003. Comparative analysis of interpolation methods in the middle Ebro Valley (Spain): application to annual precipitation and temperature. *Clim. Res.* **24**: 161–180.

- Wang XL. 2008. Penalized maximal F test for detecting undocumented mean shift without trend change. *J. Atmos. Oceanic Technol.* **25**: 368–384, doi: 10.1175/2007JTECHA982.1.
- Wang XL, Wen QH, Wu Y. 2007. Penalized maximal t test for detecting undocumented mean change in climate data series. *J. Appl. Meteorol. Climatol.* **46**: 916–931, doi: 10.1175/JAM2504.1.
- Webster R, Oliver MA. 2007. *Geostatistics for Environmental Scientists*, 2nd edn. John Wiley & Sons, Ltd: West Sussex, UK, 315 pp.
- Willmott CJ. 1982. Some comments on the evaluation of model performance. *Bull. Am. Meteorol. Soc.* **63**: 1309–1313.
- Willmott CJ, Robeson SM. 1995. Climatologically aided interpolation (CAI) of terrestrial air temperature. *Int. J. Climatol.* **15**: 221–229.
- Yatagai A, Apler P, Xie P. 2008. Development of a daily gridded precipitation data set for the Middle East. *Adv. Geosci.* **12**: 1–6.